European Journal of Chemistry

Journal webpage: www.eurjchem.com

Synthesis, characterization, anticancer activity, optical spectroscopic and docking studies of novel thiophene-2-carboxaldehyde derivatives

Mohamed Ahadu Shareef [1,*], Mohamed Musthafa [1], Devadasan Velmurugan [2], Subramani Karthikeyan [3], Singaravelu Ganesan [3], Syed Ali Padusha [4], Saiyad Musthafa [5] and Jamal Mohamed [5]

[1] *Post Graduate and Research Department of Chemistry, The New College, Chennai-600014, Tamil Nadu, India*
[2] *Centre of Advanced Study in Crystallography and Biophysics, University of Madras, Chennai-600025, Tamil Nadu, India*
[3] *Department of Medical Physics, Anna University, Chennai-600025, Tamil Nadu, India*
[4] *Post Graduate and Research Department of Chemistry, Jamal Mohamed College, Tiruchirappalli-620020, Tamil Nadu, India*
[5] *Post Graduate and Research Department of Zoology, The New College, Chennai-600014, Tamil Nadu, India*

** Corresponding author at: Post Graduate and Research Department of Chemistry, The New College, Chennai-600014, Tamil Nadu, India. Tel.: +91.97.90405029. Fax: +91.44.28352883. E-mail address: jasshaali@gmail.com (M.A. Shareef).*

ARTICLE INFORMATION

DOI: 10.5155/eurjchem.7.4.454-462.1505

Received: 31 October 2016
Accepted: 19 November 2016
Published online: 31 December 2016
Printed: 31 December 2016

KEYWORDS

Molecular docking
Anticancer activity
Drug binding pocket
Antimicrobial activity
Hydrophobic interaction
Fluorescence resonance energy transfer

ABSTRACT

2-((4-Methylpiperazin-1-yl)(thiophen-2-yl)methyl)hydrazinecarboxamide (L^1) and (2-(piperazin-1-yl(thiophen-2-yl)methyl)hydrazinecarboxamide (L^2) from the family of thiophene-2-carboxaldehyde derivatives have been synthesized. These new compounds have good antibacterial as well as antifungal activity and also less toxic in nature. Exemplary binding characteristics of these novel compounds and pharmacokinetic mechanism were confirmed by optical spectroscopic, anticancer and docking studies. The binding of thiophene-2-carboxaldehyde derivatives to carrier protein, Human Serum Albumin (HSA) has been investigated by studying its quenching mechanism, binding kinetics and the molecular distance (r) between donor (HSA) and acceptor (thiophene-2-carboxaldehyde derivatives) according to Forster's theory of non-radiative energy transfer (FRET). The micro environment of HSA has also been studied by using synchronous fluorescence spectroscopy technique and the molecular docking technique has been used to explore the hydrogen bonding, hydrophobic interaction between the human serum albumin with L^1 and L^2 compound.

Cite this: *Eur. J. Chem.* **2016**, *7(4)*, 454-462

1. Introduction

Malignancy is characterized by uncontrolled residual mutations of abnormal cells and also which leads to ultimate cell death. The International Agency for Research on Cancer (IARC) has estimated that 7.6 million individuals overall died each year as a result of tumor and 4 million individuals are affected somewhere around 30 and 69 years [1-3].

The treatment options include the use of chemotherapy for cancer patient with advanced stages, which normally involves the organization of cytotoxic operators that follow up on the procedures of cell division. The basis for this treatment methodology is that quickly partitioning malignancy cells will be more defenseless to the cytotoxic impacts of the drugs than solid onlooker cells. Normally utilized treatments, for example, doxorubicin, paclitaxel and *cis*-platin, cause serious dosage constraining symptoms because of their unfavorable consequences for the exceedingly multiplying cells in specific tissues, including the bone marrow, heart and Gastro-Intestinal tract. Therefore, it is an urgent need to develop safe and effective alternatives to the existing chemotherapy options.

Protein kinase and epidermal growth factor receptor (EGFR) are the most well-known and validated drug targets for cancer therapy. Protein kinase is the largest enzyme family involved in cell signal transduction [4-9]. They are encoded by approximately 2% of eukaryotic genes and more than 500 protein kinases, which are identified based on the human genome sequencing [10] and biochemical studies. Protein kinases catalyze exchange the γ-phosphate bunch from an ATP particle to tyrosine, serine or threonine deposits in proteins. This procedure assumes a key part in directing numerous crucial cell forms [11]. Improper activation of protein kinases are seen in a various types of cancers and in such scenarios, small molecule inhibitors are designed to target/inhibit kinase signaling [12].

ISSN 2153-2249 (Print) / ISSN 2153-2257 (Online)
http://dx.doi.org/10.5155/eurjchem.7.4.454-462.1505

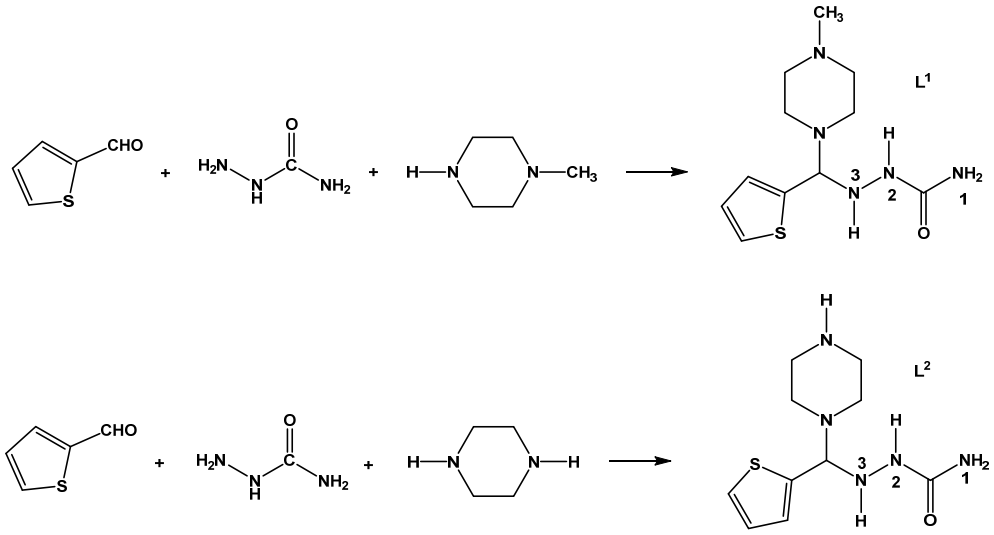

Figure 1. Synthesis of compound 2-[(4-methylpiperazin-1-yl)(thiophen-2-yl)ethyl]hydrazinecarboxamide (L^1) and 2-[piperazin-1-yl(thiophen-2-yl)methyl]hydrazinecarboxamide (L^2).

The epidermal development element receptor is derived from three auxiliary spaces: an extracellular ligand-tying area, a transmembrane area, and an intracellular space. At the point when an agonist ties to its ligand binding site, dimerization of the epidermal growth factor receptor is activated. This actuates the inborn kinase area, prompting auto phosphorylation on particular tyrosine deposits in the C-terminal [13]. Subsequently, signal transduction falls are started, which advance DNA union and cell expansion. Thus, the epidermal growth factor receptor is a factor responsible for cell relocation, bond, multiplication and resistant reactions in a few cell phenotypes in the human skin [14].

Mostly, the chemotherapeutic agents are administrated intravenously to deliver the drugs to the target organ selectively. Serum albumins are the significant local bearer found in the blood and are included in the basic carrying of exogenous and endogenous materials (unsaturated fats, supplements, steroids, and an assortment of restorative drugs). The activetion of drug mainly depends on solubility, bio-distribution and their interaction which is highly affected by their binding nature and interaction with protein. For instance, solid binding can diminish the grouping of free drugs in plasma while feeble binding might prompt poor conveyance and short lifetime [15-17]. This unmistakably demonstrates the binding of drug with protein might modify the pharmacokinetics and cytotoxic impacts. Consequently the study of the interaction of drug with protein is crucial to outline a new drug and enhance the therapeutic efficacy. Computational biology and bioinformatics play a major role in designing the drug molecules and also in speeding up the drug discovery process. Molecular docking of drug molecule with the receptor (target organ) gives important information about the drug receptor interactions.

Herein, we aim to determine the receptor interactions and binding orientation of ligand compounds by molecular docking with two proteins EGFR KINASE TKIs-L858 (PDB ID: 2ITZ) and Human Serum Albumin (HSA; PDB ID: 4L8U). Also, the human serum albumin with newly synthesized novel ligands binding kinetics was studied by fluorescence spectroscopy techniques.

2. Experimental

2.1. Reactants

Analytical grade solvents and reactants were used. *N*-Methyl piperazine, piperazine and thiophene-2-carboxaldehyde were purchased from Merck Products and used as such.

2.2. Instrumentations

Elemental analyses and characterization studies were carried out at Sophisticated Analytical Instrument Facility (SAIF), Indian Institute of Technology, Madras, Tamil Nadu and India. Melting points of synthesized compounds were measured by electric melting point apparatus SMP1. ^{1}H NMR spectra of the samples were recorded on 300 MHz using DMSO-d_6 with TMS as the internal standard. The homogeneity of the compounds was monitored by Thin Layer Chromatography (TLC) Silica-Gel coated on glass plate and visualized by iodine vapor. The absorption in the UV-Vis region was recorded by Perkin Elmer Lambda 35 Spectrophotometer using DMF/DMSO as solvents. IR spectra were recorded using KBr pellets with a Nicolet model Impact 470 FTIR spectrophotometer in the range of 4000-400 cm^{-1} at the Regional Sophisticated Instrumentation Centre, Indian Institute of Technology, Madras, Tamil Nadu, India, using tetracyanoethylene (TCNE) as the internal standard. Anti-cancer and cytotoxic studies were carried out at Royal Bio Research Centre, Velachery, Chennai, Tamil Nadu and India.

2.3. Synthesis

Thiophene-2-carboxaldehyde, *N*-methylpiperazine and semicarbazide hydrochloride were taken in 1:1:1 mol ratio and allowed to react as shown in Figure 1. Semicarbazide (11.2 g, 0.1 mol) was taken in a round bottom flask and 10 mL of water was added. To this solution 10.0 mL (0.1 mol) *N*-methyl piperazine was added and stirred well for 15 min by keeping the reaction mixture on a magnetic stirrer. Thiophene-2-carboxaldehyde (9.3 mL, 0.1 mol) was added to the above mixture and stirring was continued under ice cold condition. The colorless solid formed was filtered, washed and recrystallized using ethanol. The same procedure was followed for the synthesis of the rest of the compounds as shown in Figure 1 [18-22].

2-((4-Methylpiperazin-1-yl)(thiophen-2-yl)methyl)hydrazinecarboxamide (**L^1**): Yield: 53%. M.p.: 150-152 °C. FT-IR (KBr, ν, cm^{-1}): 3301 (N^1H_2), 1548 (NH, amide II band), 1622 (C=O, amide I band). ^{1}H NMR (400 MHz, $CDCl_3$, δ, ppm): 7.88 (s, 2H,

NH_2), 7.45-7.44 (m, 3H,thiophene), 7.13 (d, 1H, NH(C=O)), 4.15 (s, 1H, CH(NH)), 3.90 (s, 3H, CH_3 (piperazine)), 2.51-2.50 (m, 8H, piperazine), 1.92 (s, 1H, NH(CH)). ^{13}C NMR (100 MHz, $CDCl_3$, δ, ppm): 172.45, 150.02, 132.26, 130.13, 121.89, 114.97, 56.15. HRMS (ESI, *m/z*) calcd. for $C_{11}H_{19}N_5OS$ [M-H]:269.13; Found: 269.2312. Anal. calcd. for $C_{11}H_{19}N_5OS$: C, 49.05; H, 7.11; N, 26.00. Found: C, 49.08; H, 7.08; N, 26.01%.

2-(Piperazin-1-yl(thiophen-2-yl)methyl) hydrazinecarboxamide (**L²**): Yield: 52%. M.p.: 149-153 °C. FT-IR (KBr, ν, cm^{-1}): 3245 ν(N^1H_2), 3153 ν(N^2H), 1599 δ(N^3H), 1719 (C=O). ^{1}H NMR (400 MHz, $CDCl_3$, δ, ppm): 9.95 (s, 2H, NH_2), 7.85 (s, 1H, NH), 7.13 (m, 3H, Thiophene), 4.18 (s, 1H, CH), 2.56 (m, 8H, piperazine), 2.40 (d, 1H, NH (CH)), 1.92 (s, 1H, NH of piperazine). ^{13}C NMR (100 MHz, $CDCl_3$, δ, ppm): 170.26, 150.02, 139.75, 130.18, 129.79, 121.89, 114, 99, 40.50, 40.00. HRMS (ESI, *m/z*) calcd. for $C_{10}H_{17}N_5OS$ [M-H]: 255.12; Found: 255.3000. Anal. calcd. for $C_{10}H_{17}N_5OS$: C, 47.04; H, 6.71; N, 27.43. Found: C, 47.08; H, 6.08; N, 26.22%.

2.4. Antimicrobial studies

2.4.1. Antibacterial activity

To study the antibacterial activity of newly synthesized compounds, nutrient agar was used as a medium. The agar medium was prepared by dissolving 5 g of yeast extract, 10 g meat extract, 5 g of peptone, 5g of sodium chloride and 20 g of agar in 100 mL of distilled water in a clean conical flask and the pH was maintained at 7. The solution was boiled to dissolve the medium completely and sterilized by autoclaving at 7 kg pressure (121 °C) for 15 minutes. After sterilization 20 mL media was poured in to the sterilized petri plates. These petri plates were kept at room temperature for some time. After a few minutes, the medium got solidified in the plate. Then, it was incubated for 12 h. After the incubation, it was inoculated with microorganisms, using simile swabs. All these manipulations were carried out with atmospheric air under aseptic condition.

2.4.2. Antifungal activity

The potato dextrose agar (PDA) is used as a medium to determine antifungal activity of newly synthesized ligands. The PDA was prepared by dissolving 20 g of potato extract, 20 g of agar and 20 g of dextrose in one liter of distilled water in a clean conical flask. The solution was boiled to dissolve the media completely and sterilize by autoclaving with 7 kg pressure (121 ℃) for 30 minutes. After sterilization, 20 mL media was poured into the sterilized petri plates. These petri plates were kept at room temperature for some time. After a few minutes, the medium gets solidified in the plate.0.5 mL of DMSO was used as solvent and 10μg of Amphotericin B as control. In a typical procedure, a well-made agar medium was inoculated with microorganism and it was filled with 50μL of test solution using a micro pipette. Later, the plates were incubated at 35 °C for 72 h. During this period, the test solution diffuses and affects the growth of the inoculated.

2.5. Human serum albumin (HSA)

Human serum albumin (HSA) was purchased from Hi Media laboratory Pvt. Limited, Mumbai, India and it was used without any further purification. Millipore water was used for preparing solution throughout the experiments. HSA solution was prepared in phosphate buffer solution of pH = 7.4. HSA solution was kept in the dark at 4 °C. L^1 and L^2 are newly synthesized compounds, and the stock solutions of these derivatives were also prepared using the same buffer.

2.6. Fluorescence spectroscopy studies

The steady states fluorescence emission measurements were obtained using a commercially available spectrofluorometer (Fluoromax-2, ISA; Jobin-Yuvon-Spex, Edison, NJ) and spectral band passes were kept at 5 nm in both excitation and emission monochromators. The emission spectrum was recorded in the wavelength region 300-540 nm at 280 nm excitation. Synchronous fluorescence spectra were recorded by simultaneously scanning the excitation (λ_{ex}) and emission (λ_{em}) monochromators with two different constant wavelength intervals (Δλ) such as 15 and 60 nm between the excitation and emission monochromators. This was carried out with the help of Fluoromax-2 equipped with an excitation source (150W ozone free Xenon arc lamp) coupled to the monochromatic delivering light to the sample spot at desired wavelength. The fluorescence emission from the sample was collected by an emission monochromatic to photomultiplier tube (R928; Hamamatsu, Shizuoka-Ken, Japan). In addition, using the absorption spectrum of L^1 and L^2 fluorescence spectrum of HSA (concentration ratio of drug and protein is 1:1 at pH = 7.4), the fluorescence resonance energy transfer and energy transfer efficacy of HSA with various concentration of drug were also evaluated.

2.7. Molecular docking studies

Molecular docking is a powerful tool in understanding different protein functions. The X-ray crystal structures of the Protein EGFR KINASE TKIs - L858 (2ITZ) and human serum albumin protein (Monomer with 585 amino acids) (PDBID: 4L8U) obtained from protein data bank database. Energies of protein structures were minimized using protein preparation wizard panel to include hydrogens [23-25]. The charge state of protein residues is important for result generation by Glide. Optimized potential of liquid simulations (OPLS) force field was used for minimization process. Protein preparation facility consists of two steps, preparation and refinement. Energy minimization reorients side-chain hydroxyl groups and alleviates potential steric clashes. These structures were energy minimized using two algorithms with steepest descent and conjugate gradient. Compounds were docked in two drug binding sites using the induced fit docking (IFD) protocol. Here, both the ligand and protein are flexible to dock, and hence many conformations are generated for an individual ligand. Based on the docking score, glide energy and hydrogen bond interaction, the best conformation is sorted and results were analyzed.

3. Results and discussion

3.1. Synthesis

Physicochemical characterization of the synthesized compounds were done by the analytical methods such as melting point, TLC, elemental analysis, and spectral methods such as UV-Visible, IR, ^{1}H NMR, ^{13}C NMR and Mass, Figure 2.

3.2. Antimicrobial studies

Agar well dispersion strategy was applied to determine the antibacterial and antifungal activities of these novel compounds. All blended mixtures were screened for their *in-vitro* antifungal movement against *Candida albicans*, *Penicillium notatum* and *Aspergillus flavus* and *in-vitro* antibacterial action against Gram-negative *Escherichia coli*, Gram-positive *Staphylococcus aureus*, *Vibrio para haemolyticus*, *Bacillus subtilis*, *Klebsiella* and *Pseudomonas aeruginosa.* Amphotericin (20 μg/plate) and streptomycin (20 μg/circle) were utilized as standard references for antibacterial and antifungal activity, respectively.

Table 1. Antimicrobial studies of compound L^1.

Compound	Zone of inhibition (mm)									
	Bacteria						Fungi			
	S. aureus	*B. subtilis*	*V. parahaemolyticus*	*E. coli*	*Klebsiella*	*P. aeruginosa*	*C. albicans*	*A. niger*	*A. Flavus*	*P. notatum*
TNS	16	10	10	7	7	9	9	8	8	11
Streptomycin	20	11	13	7	6	7	-	-	-	-
Amphotericin	-	-	-	-	-	-	6	7	8	9
Solvent	-	-	-	-	-	-	-	-	-	-

Table 2. Antimicrobial studies of compound L^2.

Compound	Zone of inhibition (mm)									
	Bacteria						Fungi			
	S. aureus	*B. subtilis*	*V. parahaemolyticus*	*E. coli*	*Klebsiella*	*P. aeruginosa*	*C. albicans*	*A. niger*	*A. Flavus*	*P. notatum*
TNS	15	10	8	7	5	5	4	6	6	8
Streptomycin	20	11	13	7	6	7	-	-	-	-
Amphotericin	-	-	-	-	-	-	6	7	8	9
Solvent	-	-	-	-	-	-	-	-	-	-

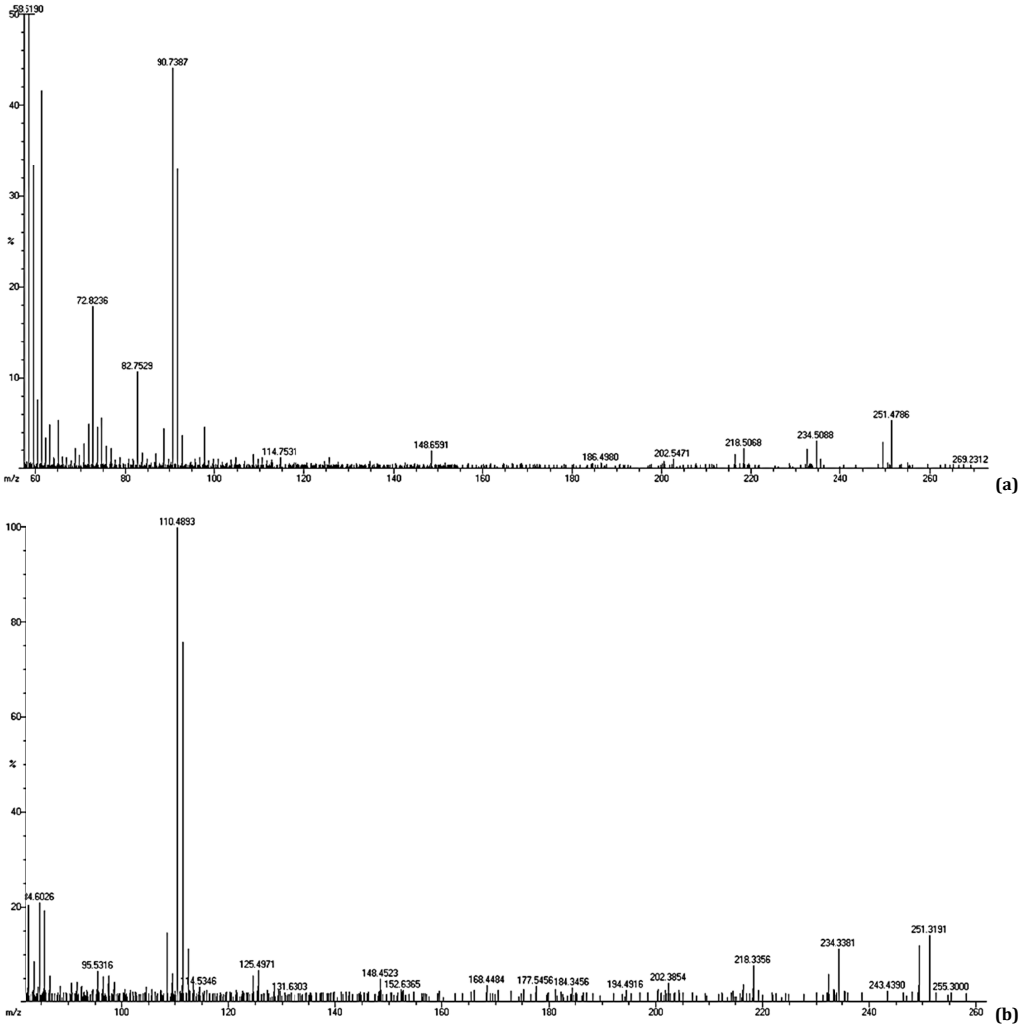

Figure 2. Mass spectrum of compound L^1 and L^2.

After hatching, the distance across of the zone of hindrance conformed to the depressions and plate of standard medications were precisely measured in mm. The observed zones of inhibition are presented in Table 1 and 2. Both compounds showed significant antibacterial activity but weak to moderate antifungal activity. L^1 and L^2 exhibited good antibacterial activity comparable with standard drug while L^2 bearing amide moiety showed moderate antifungal activity. L^1 exhibited comparable activity against all tested fungal strains and showed good zone of inhibition against *Candida albicans* and *Penicillium notatum* while L^2 showed weak zone of inhibition against all the selected fungal strains.

3.3. Fluorescence spectroscopy studies

The binding affinities of drug and protein interaction mechanism were carried out by using fluorescence emission spectroscopy.

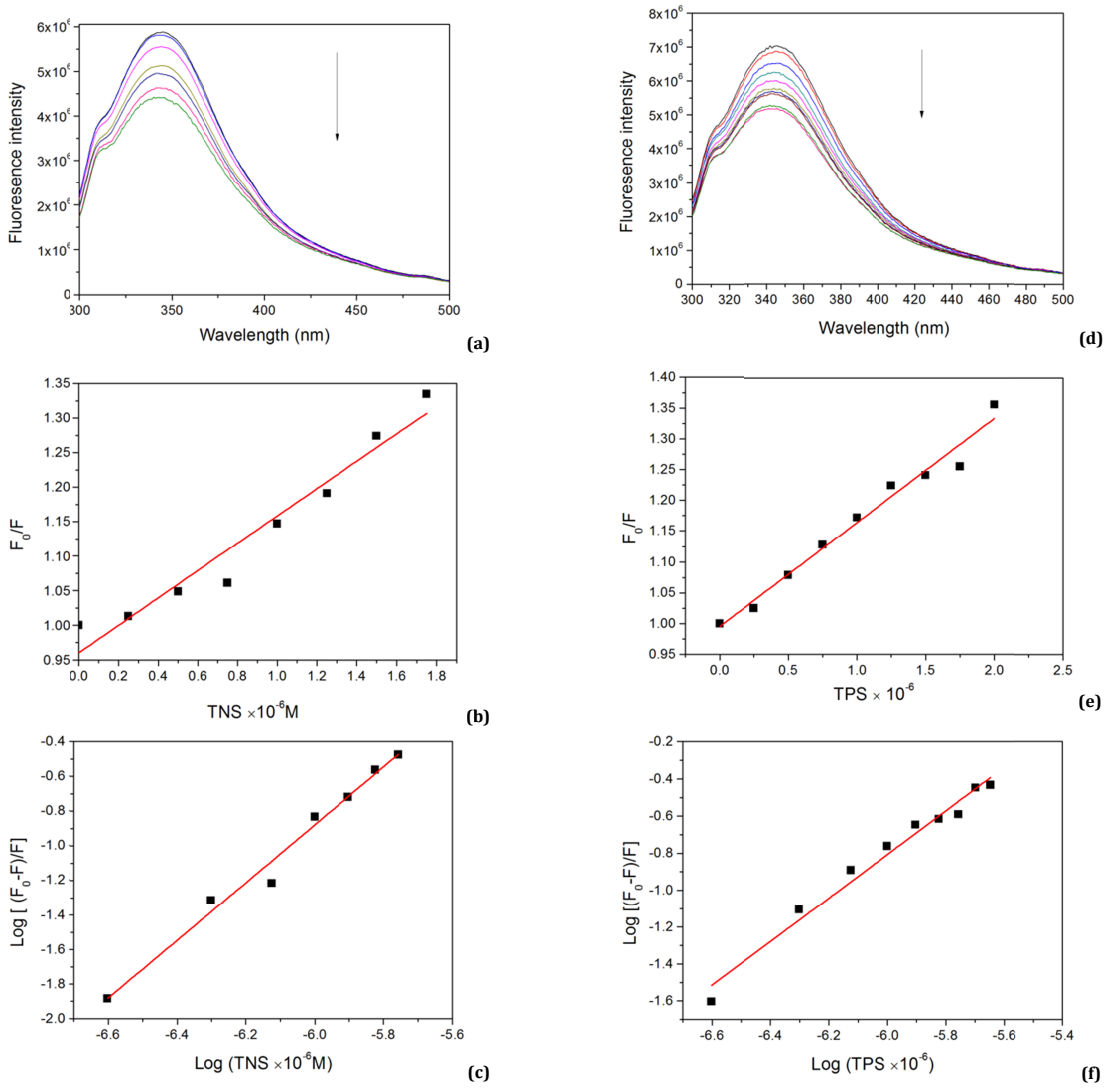

Figure 3. Fluorescence emission spectra of HSA-L^1 (a), HSA-L^2 (d) (pH = 7.4). HSA (0.1×10^{-5} M) in the presence of L^1, L^2 (0 to 2×10^{-5} M), respectively. Stern-Volmer plot [L^1 (b), L^2 (e)]. The plot of log (F_0-F)/F versus Log [Q] [L^1(c), L^2(f)].

The HSA emission spectrum comes from tryptophan, tyrosine, and phenylalanine amino acid residues. Small molecules when bound to HSA would change the intrinsic fluorescence intensity due to the tryptophan residue. Titration of different concentrations of compound L^1 and L^2 (0-2 μM) to HSA resulted in a decrease in the fluorescence maximum emission at 347 and 349 nm, respectively (Figure 3a and 3d) and the shape of the peaks remained almost unchanged. Hence this decrease in fluorescence intensity due to the interaction of fluorophore with in protein local environment, and also the fluorescence quenching of HSA depend on the concentration of both the drugs. Here, both the drugs (compound L^1 and L^2) act as quencher and bind in the vicinity of Trp214 leading to a decrease in the fluorescence emission. These results indicate that, upon binding of compound L^1 and L^2 drugs into the HSA, the HSA complex was formed.

To estimate the nature of the quenching phenomenon Stren-Volmer equation is used.

$$F_0 / F = 1 + K_{SV}[D] = 1+Kq[D]; \qquad Kq = Ksv/\tau_0 \qquad (1)$$

where F_0 and F are the fluorescence intensities before and after the addition of the quencher, K_{SV} is the dynamic quenching constant; Kq is the quenching rate constant; [D] is the concentration of the quencher; τ_0 is the average life time of the molecule without quencher and its value is considered to be 1×10^{-8} s.

The Stern-Volmer plots of the quenching of HSA fluorescence by compound L^1 and L^2 are shown in Figure 3b and 3e. Stern-Volmer quenching constants K_q were 1.291×10^{13} and 1.578×10^{13} L/mol. The results showed K_q to be much greater than the limiting diffusion rate constant of both the macromolecular complexes (2.0×10^{10} L/mol), which indicates that probable quenching mechanism of HSA-Compound L^1 and L^2 interaction was initiated and this may be due to static quenching [26].

3.4. Binding constant and the number of binding sites

The binding constant K_a and the quantity of binding destinations can be ascertained utilizing the accompanying mathematical statement [27].

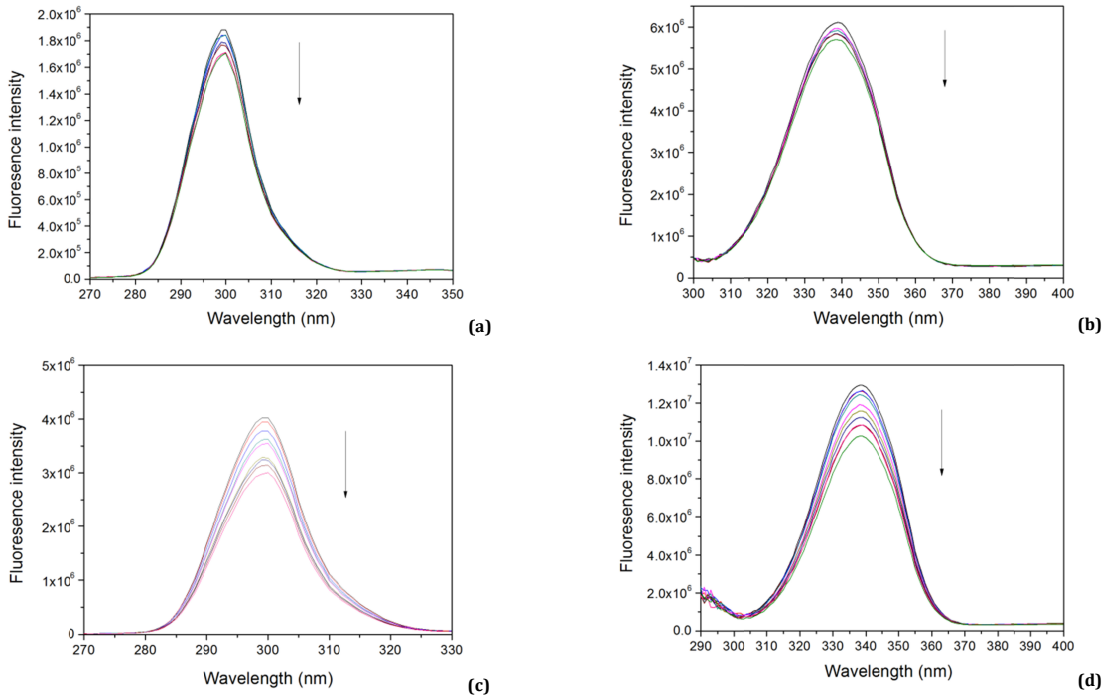

Figure 4. Synchronous fluorescence and its spectra, at Δλ = 15 nm [L¹ (a), L²(c)] and Δλ = 60 nm [TNS (b), TPS (d)]) of HSA (0.1×10^{-5} M) in the presence of (0-2 μM) L¹ and L², respectively.

$$\text{Log}\,[(F_0/F)/F] = \text{Log}\,K_a + n\,\text{Log}\,[D] \quad (2)$$

A plot of log $[(F_0\text{-}F)/F]$ *vs* log [D] gives a straight line (Figure 3c and 3f) of HSA compound with compound L¹ and L². From the plot we can obtain the binding constant K_a = 9.13×10^5 L/mol and 6.25×10^5 L/mol. and binding site for the two compounds n = 1.3 and 1.1 respectively. The results show that there is one class of binding site for drug in HSA and drugs could be bound and transported by HSA to the body.

3.5. Synchronous fluorescence spectroscopy

Synchronous fluorescence spectra of HSA with different concentrations of compound L¹ (Figure 4a and 4c) and compound L² (Figure 4b and 4d) were measured to explore the conformational changes of HSA. The synchronous fluorescence spectra give the information about the molecular environment in the region of the chromospheres of molecules, and change in the maximum emission wavelengths which indicate the conformational changes of HSA. The excitation wavelength and emission wavelengths were located at Δλ = 15 and 60 nm and the synchronous fluorescence spectra give the characteristic information about tyrosine and tryptophan residues, respectively [28] for both the compound L¹ and L² with HSA complex. The quenching of the fluorescence intensity of tyrosine residue is better when compared to tryptophan residue, which shows that tyrosine residue contributes incredibly to the natural fluorescence of HSA for both compound L¹ and L². Inconsiderable blue shift in the fluorescence emission which indicates maximum of tyrosine residue was noticed after the addition of both compound L¹ and L². But the maximum emission of tryptophan remained unchanged.

3.6. Energy transfer from HSA to compound L¹and L²

Forster resonance energy transfer (FRET) is an effective apparatus to decide the separation between two points in proteins (donor and an acceptor) furthermore FRET distance between the points have been broadly used to contemplate the conformational changes upon ligand binding and protein-protein associations. According to the Forster non-radiative energy transfer theory, the energy transfer should happen at the following conditions: (1) The donor should have more fluorescence quantum yield, (2) The overlap should be >30% of the fluorescence emission spectrum of the donor with the absorption spectrum of the acceptor (3) The distance between the donor and acceptor is within 8 nm. Energy transfer efficiency E is defined by the following equation.

$$E=1-(F/F_0) \quad (3)$$

where F is the fluorescence intensity of the donor in the presence of acceptor and F_0 is the fluorescence intensity of the donor. The fluorescence intensity of HSA is reduced by the energy transfer to compound L¹ and L². The energy transfer efficiency is related to distance between the acceptor and donor distance and critical energy transfer distance (R_0).

$$E = \frac{R_0^6}{(R_0^6+r^6)} \quad (4)$$

where R_0 is the critical distance when the transfer efficiency is 50% and r is the binding distance between the donor and acceptor.

$$R_0 = 8.79\times10^{-25}[k^2N^{-4}\varphi_D J] \quad (5)$$

where k^2 is the spatial orientation factor of the dipole, N is the average refractive index of water, φ_D is the quantum yield of the donor in the absence of the acceptor. J is the overlap integral of the fluorescence emission spectrum of the donor and the absorption spectrum of the acceptor in units $M^{-1}cm^3$. J is given by following equation

$$J(\lambda) = \int_0^\infty F_D(\lambda)\varepsilon_A(\lambda)\lambda^4 d\lambda \quad (6)$$

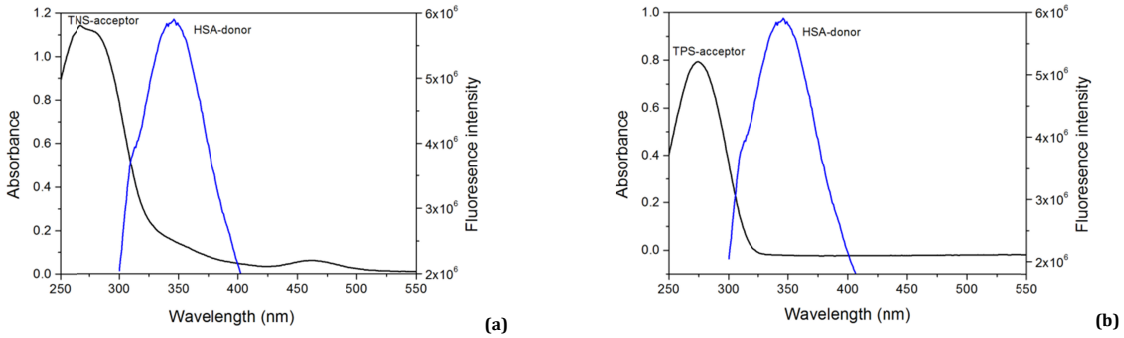

Figure 5. The overlap of the fluorescence emission spectrum of HSA and the absorption coefficient spectrum of L^1 (a) and L^2 (b).

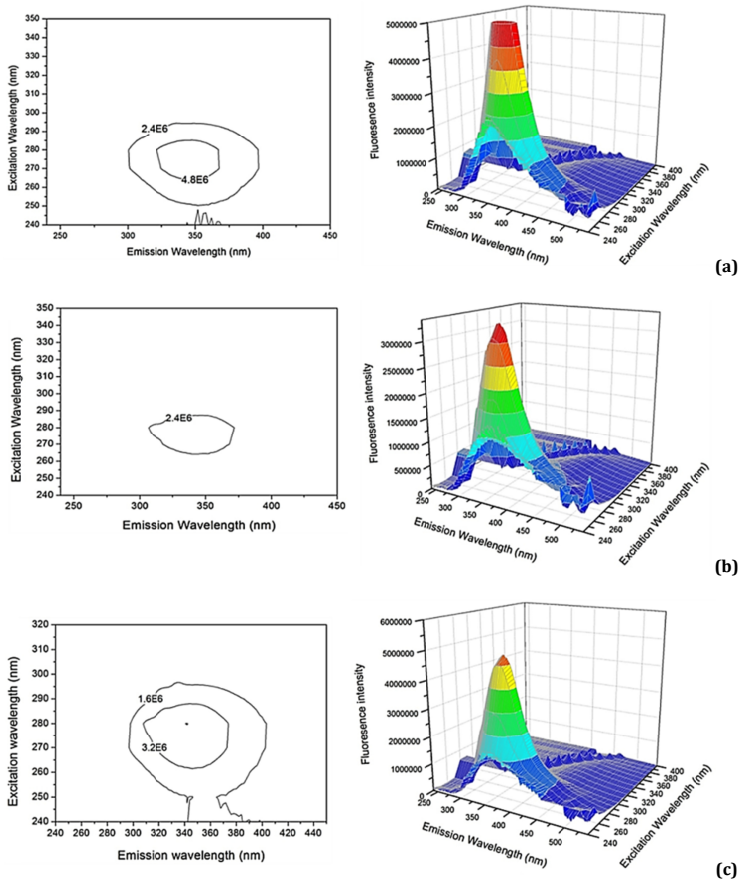

Figure 6. The fluorescence contour maps of (a) HSA, (b) L^1-HSA and (c) L^2-HSA. Concentration of HSA is 1 μM and L^1, L^2 are 2 μM.

where F_D (λ) is the fluorescence intensity of the donor at wavelength λ to λ + Δλ, with the total intensity normalized to unity and ε_A (λ) is the molar extinction coefficient of the acceptor at wavelength (λ). Figure 5 shows considerable overlap to the fluorescence emission spectrum of HSA with absorption spectrum of both compounds L^1 (Figure 5a), and L^2 (Figure 5b). From the overlapping of the absorption spectrum of the acceptor and fluorescence spectrum of the donor we can calculate the J value of both compound L^1 and L^2 as 2.4148 × 10^{-19} $M^{-1}cm^3$, 1.2148 × 10^{-20} $M^{-1}cm^3$ and the value of R_0 = 0.406 nm, 0.247 nm, E = 0.109, 0.146, k^2 = 2/3, N = 1.336 and φ_D=0.118, r=0.577 nm, 0.331 nm. Both R_0 and r values are lower than the maximum standard values for R_0 (< 10 nm) and the donor and acceptor distance r < 8 nm. So, there is possibility of energy transfer between HSA and compound L^1 and L^2 [29,30].

3.7. Three dimensional fluorescence spectroscopy studies

The three dimensional spectra is a powerful method to study the conformational changes of protein and additionally it can give add up to data with respect to the fluorescence qualities by changing the excitation emission wavelength at the same time. The excitation, emission florescent spectra of HSA, HSA-compound L^1 and HSA-compound L^2 complex are shown in Figure 6a-c, respectively. As shown in the figure, the fluorescent intensity of peak decreased with addition of drug (L^1 and L^2) in all systems and the possible reason is due to complex formation between drug and protein.

Table 3. Glide energy docking score of human lung cancer protein (PDB ID: 2ITZ), human serum albumin (PDB ID: 4L8U) with compound L^1 and L^2.

Compound	Dock score (Kcal/mol)	Glide energy (Kcal/mol)	Hydrogen bond (D-H...A)	Distance (Å)
Glide energy docking score of human lung cancer protein (PDB ID: 2ITZ) with L^1 and L^2				
L^1	-6.496	-43.713	ARG 841 & ASP 855	<1.7
L^2	-6.106	-42.542	ARG 841 & ASP 855	<1.7
Glide energy docking score of human serum albumin (PDB ID: 4L8U) with L^1 and L^2				
L^1	-5.002	-44.670	LEU 115 & ARG 114 (A)	<3.0
L^2	-3.023	-43.124	LEU 115 & ARG 117(A)	<3.0

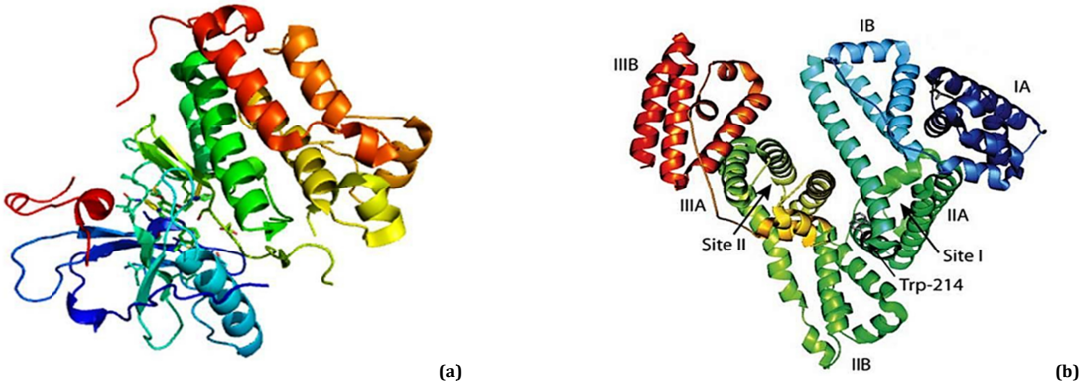

Figure 7. Crystal structure of (a) EGFR-Kinase domain l858r mutation in complex with iressa (PDB ID: 2ITZ) (b) Human serum albumin complexed with 9 amino camptothecin.

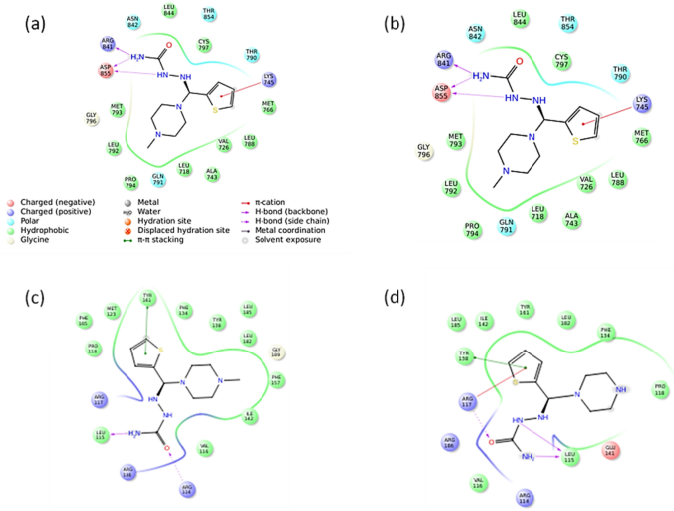

Figure 8. LIGPLOT for EGFR kinase domain (a) L^1 (b) L^2 and human serum albumin (c) L^1 (d) L^2 complex.

The result indicates that fluorescent intensities of HSA-compound L^1, HSA-compound L^2 complexes were lower than that in free HSA, in which the polarity around both residues, *Trp* and *Tyr* may be reduced. This means that the binding site between HSA and the drug is located within this hydrophobic pocket. The decrease of fluorescence emission intensity of this peak together with the synchronous fluorescence result reveals that the interaction of drug (L^1 and L^2) with HSA induced some changes in the micro-environment and the confirmation of protein [31-33].

3.8. Molecular docking study

Molecular docking studies of synthesized ligand complexes were carried out using Maestro Version 9.3.5. as docking programme so as to support bioorganic movement results and to understand in subtle elements, the different interaction in the middle of ligand and protein at the active site of residues. The X-ray crystal structure of human lung cancer protein (PDB ID: 2ITZ) (Figure 7a) and human serum albumin protein (PDBID: 4L8U) were used for docking study (Figure 7b). The 'Site Finder' tool of the program was used to search for its active site. Docking procedures were performed for each ligand and the best conformation of each of the ligand receptor complexes was selected based on energetic grounds. The affinity scoring function ΔG was used to assess and rank the receptor ligand complexes. The docking scores and the hydrogen bonding strength of L^1 and L^2 are shown in Table 3. In the overall molecular interaction of the ligands L^1 and L^2 with human lung cancer protein (Figure 8a (L^1) and 8b (L^2)) and human serum albumin (Figure 8c (L^1) and 8d (L^2)) which were shown together in Figure 8. It is found out that docking score is very minimal as the binding interaction forces of both human serum albumin and human lung cancer protein results revealed that the ligands have potential binding capacity and anticancer activity.

4. Conclusions

In the present study, the amide is an important functional group and due to its electron properties, it is able to interact and bind with a number of receptors. Therefore, the reason for the wide spread occurrence of amides in modern pharmaceuticals and biologically active compounds is obvious. The properties of the amide moiety can be easily modified by various substitutions. Thus the presence of an amide-like moiety is characteristic for various anticancer, antibacterial and antifungal agents. We have performed antimicrobial activity and the results showed very potent activity against many Gram positive and negative microbes and the binding interactions of ligands and amino acids receptors were experimentally confirmed with docking scores. Presently we have made an attempt to determine the molecular interactions of ligands and protein receptors using molecular docking studies and optical spectroscopic fluorescence studies.

Acknowledgements

The authors would like to express their gratitude to the Head, Department of Chemistry, Principal and Management committee of The New College, for providing necessary facilities. We are thankful to Sophisticated Analytical Instrument Facility (SAIF), Indian Institute of Technology - Chennai for compound characterization studies, Department of Biotechnology supported Bioinformatics Infrastructure Facility, University of Madras for molecular docking studies and Royal Bio Research Centre, Velachery, Chennai for Technical Support, Fluorescence spectroscopy study was supported. We also thank the Board of Research in Nuclear Sciences, Department of Atomic Energy, Government of India, for permitting us to carry out Fluorescence Spectroscopy study.

References

[1]. Bray, F.; Ren, J. S.; Masuyer, E.; Ferlay, J. *Cancer*. **2013**, *132(5)*, 1133-1145.
[2]. Ferlay, J.; Soerjomataram, I.; Ervik, M.; Dikshit, R.; Eser, S.; Mathers, C.; Rebelo, M.; Parkin, D.M.; Forman, D.; Bray, F. GLOBOCAN 2012 v1.0, Cancer Incidence and Mortality Worldwide: IARC CancerBase No. 11, Lyon, France: International Agency for Research on Cancer, Available from http://globocan.iarc.fr
[3]. Blume-Jensen, P.; Hunter, T. *Nature***2001**, *411(6835)*, 355-365.
[4]. Hunter, T. *Cell*. **2000**, *100(1)*, 113-127.
[5]. Stevens, L. A.; Levey, A. S. *J. Am. Soc. Nephrol.* **2009**, *20(11)*, 2305-2313.
[6]. Coresh, J.; Astor B. C.; Greene, T.; Eknoyan, G.; Levey, A. S. *Am. J. Kidney Dis.* **2003**, *41(1)*, 1-12.
[7]. Cockcroft, D. W.; Gault M. H. *Nephron*. **1976**, *16(1)*, 31-41.
[8]. Levey, A. S.; Coresh, J.; Greene, T. *Ann. Intern. Med*. **2006**, *145(4)*, 247-254.
[9]. Manning, G.; Whyte, D. B.; Martinez, R.; Hunter, T.; Sudarsanam, S. *Science* **2002**, *298(5600)*, 1912-1934.
[10]. Jorissen R. N. *Exp. Cell Res.* **2003**, *284(1)*, 31-53.
[11]. Ciardiello, F. *Curr. Opin. Oncol.* **2004**, *16(2)*, 130-135.
[12]. Citri, A.; Yarden, Y. *Nat. Rev. Mol. Cell Biol.* **2006**, *7*, 505-516.
[13]. Downward, J.; Parker, P.; Waterfield, M. D. *Nature* **1984**, *311*, 483-485.
[14]. Oda, K.; Matsuoka, Y.; Funahashi, A.; Kitano, H. *Mol. Syst. Biol.* **2005**, *1*, E11-E17.
[15]. Zhang, H.; Berezov, A.; Wang, Q.; Zhang, G.; Drebin, J.; Murali, R. *J. Clin. Invest.* **2007**, *117*, 2051-2058.
[16]. Olson, R. E.; Christ, D. D. *Annu. Rep. Med. Chem.* **1996**, *31*, 327-337.
[17]. Belinelo, V. J.; Reis, G. T.; Stefani, G. M.; Ferreira-Alves, D. L.; Pilo-Veloso, D. *J. Brazilian Chem. Soc.* **2002**, *13(6)*, 830-837.
[18]. Rizwan-Sulthana, A.; Padusha, S. A. M.; Jameel, A. A. *Indian J. Sci. Commun.* **2012**, *5(1)*, 55-58.
[19]. Valarmathi, R.; Akilandeswari, S.; Indulatha, V. N.; Umadevi, G. *Der Pharm. Sinica* **2011**, *2(5)*, 64-68.
[20]. Raman, N.; Thangaraja, C.; Raja, S. J. *Indian J. Chem. A* **2005**, *44*, 693-699.
[21]. Abdul-Jameel, A.; Palanisamy, M.; Syed Ali Padusha, M. *Der Chemica Sinica* **2012**, *3(4)*, 860-863.
[22]. Abdul-Jameel, A.; Padusha, S. A. M. *Asian J. Chem.* **2011**, *23(3)*, 1260-1262.
[23]. Gao, H.; Lei, L.; Liu, J.; Kong, Q.; Chen, X.; Hu Z. *J. Photochem. Photobiol. A: Chem.* **2004**, *167*, 213-221.
[24]. Zhu, K.; Day, T.; Warshaviak, D.; Murrett, C.; Friesner, R.; Pearlman, D. *Proteins: Struct., Funct., Bioinf.* **2014**, *82*, 1646-1655.
[25]. Schrödinger Release 2014-1, Schrödinger Suite 2014-1 Protein Preparation Wizard; Epik version 2.7, Schrödinger, LLC, New York, NY, 2013; Impact version 6.2, Schrödinger, LLC, New York, NY, 2014; Prime version 3.5, Schrödinger, LLC, New York, NY, 2014.
[26]. Karthikeyan, S.; Chinnathambi, S.; Kannan, A.; Rajakumar, P.; Velmurugan, D.; Bharanidharan, G.; Aruna, P.; Ganesan, S. *J. Biochem. Mol. Toxicol.* **2015**, *29*, 373-381.
[27]. Karthikeyan, S.; Chinnathambi, S.; Velmurugan, D.; Bharanidharan, G.; Ganesan, S. *Nano Biomed. Eng.* **2015**, *7*, 1-7.
[28]. Karthikeyan, S.; Bharanidharan, G.; Kesherwani, M.; Karthik, A. M.; Srinivasan, N.; Velmurugan, D.; Aruna, P.; Ganesan, S. *J. Biomol. Str. Dyn.* **2015**, *34(6)*, 1264-1281.
[29]. Li, Z.; Jiao, G.; Sun, G.; Song, L.; Sheng, F. *J. Biochem. Mol. Toxicol.* **2012**, *26(9)*, 331-336.
[30]. Zhang, Y. Z.; Zhou, B.; Liu, Y. X.; Zhou, C. X.; Ding, X. L.; Liu, Y. J. *Fluoresc*. **2008**, *18(1)*, 109-118.
[31]. Huang, C. Z.; Lu, W.; Li, Y. F.; Huang, Y. M. *Anal. Chim. Acta.* **2006**, *556(2)*, 469-475.
[32]. Hu, Y. J.; Liu, Y.; Wang, J. B.; Xiao, X. H.; Qu, S. S. *J. Pharm. Biomed. Anal.* **2004**, *36(4)*, 915-919.
[33]. Chinnathambi, S.; Velmurugan, D.; Hanagata, N.; Aruna, P.; Ganesan, S. *J. Lumin.* **2014**, *151*, 1-10.